Progress In Electromagnetics Research M, Vol. 11, 89–98, 2010

FINITE-DIFFERENCE FREQUENCY-DOMAIN ANALYSIS OF LINEAR ARRAYS OF DIELECTRIC CYLINDERS WITH THE ADAPTIVE BASIS FUNCTIONS/DIAGONAL MOMENT MATRIX TECHNIQUE

G. Zheng, B.-Z. Wang, and X. Ding

Institute of Applied Physics
University of Electronic Science and Technology of China
Chengdu 610054, China

Abstract—The finite-difference frequency-domain (FDFD) method with the adaptive basis functions/diagonal moment matrix (ABF /DMM) technique is proposed in this paper for finite periodic linear arrays of inhomogeneous dielectric cylinders, in which the versatility of the FDFD method and the high efficiency of the ABF/DMM technique are combined. The method in this paper and the classical full-domain FDFD method are compared in the given numerical examples. The results obtained by the two methods respectively are in good agreement, but the computational times are largely reduced in the method in this paper.

1. INTRODUCTION

The finite-difference frequency-domain (FDFD) method is very flexible to analyze complicated problems and has been widely used in numerical simulations [1–6]. In the classical full-domain FDFD method, the whole computational domain needs to be discretized with Yee's cells [7] and then truncated by a boundary condition like Mur's absorbing boundary condition, perfect matched layer (PML), etc. Boundary integral equation as a global absorbing boundary condition was applied to the FDFD method [2] which allows the boundary to be very close to a scattering surface. But the global absorbing boundary condition based on boundary integral equation results in dense matrix blocks in the final matrix equation, which largely increases the burden of computation and storage. This demerit becomes very serious when

Corresponding author: G. Zheng (zhenggang@uestc.edu.cn).

a large scattering object is analyzed, such as a large array, so some efficient techniques must be adopted.

Boundary integral equation not only can be applied as an absorbing boundary condition, but also can be used to set up the relationship between the FDFD method and the method of moment (MoM), which allows some efficient techniques for the MoM to be used for the FDFD method. The adaptive basis functions/diagonal moment matrix (ABF/DMM) technique as an efficient technique was proposed for the MoM [8]. Then it was used to analyze problems of arrays [9]. The final matrix equation of the MoM with this technique is highly diagonally dominant and can be solved by an iterative algorithm efficiently.

In this paper, the combining scheme of the FDFD method and the ABF/DMM technique are given for analyzing finite periodic linear arrays of inhomogeneous dielectric cylinders, so that both the versatility of the FDFD method and the high efficiency of the ABF/DMM technique can be utilized. The FDFD method with the ABF/DMM technique is described in Section 2 in detail. Some numerical results obtained by the method in this paper are given and compared with those obtained by the classical full-domain FDFD method in Section 3. Finally, the work of this paper is concluded in Section 4.

2. FORMULATION

A finite periodic linear cylinder array is shown in Figure 1, which has M_e elements. These elements are included in M_e sub-domains, respectively. A boundary integral equation is set up on the boundaries of these sub-domains which are close to the surfaces of elements.

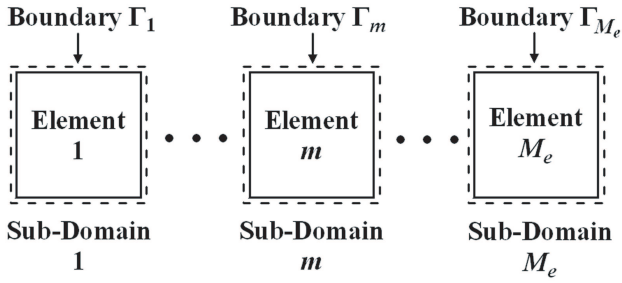

Figure 1. A finite periodic linear cylinder array with M_e elements, which are included in M_e sub-domains respectively.

2.1. Boundary Integral Equation

Here, the case of TE wave is considered, and the case of TM wave can be handled in a similar way. Equation (1) should be satisfied on the boundary Γ:

$$H_z^{inc}(\boldsymbol{\rho}) = H_z^t(\boldsymbol{\rho}) - \oint_\Gamma H_z^t(\boldsymbol{\rho}') \frac{\partial G(\boldsymbol{\rho}, \boldsymbol{\rho}')}{\partial \mathbf{n}'} d\Gamma' + \oint_\Gamma \frac{\partial H_z^t(\boldsymbol{\rho}')}{\partial \mathbf{n}'} G(\boldsymbol{\rho}, \boldsymbol{\rho}') d\Gamma'$$

$$\boldsymbol{\rho} \text{ on } \Gamma \quad (1)$$

where H_z^t is the z-component of the total magnetic field. H_z^{inc} is the z-component of the incident magnetic field. $G(\boldsymbol{\rho}, \boldsymbol{\rho}')$ is the two-dimensional Green function in free space. $\boldsymbol{\rho}$ and $\boldsymbol{\rho}'$ are position vectors. Γ is the boundary of all sub-domains and equal to $\Gamma_1 \cup \Gamma_2 \cup \ldots \cup \Gamma_{M_e}$, where Γ_m is the boundary of Sub-domain m. $\mathbf{n}$ is normal to Γ and outward of the sub-domains, and $\frac{\partial}{\partial \mathbf{n}'}$ is $\mathbf{n}$-directional derivative with regard to $\boldsymbol{\rho}'$. H_z^t and $\frac{\partial H_z^t}{\partial \mathbf{n}}$ on the boundary Γ can be represented with rectangular pulse functions as follow:

$$H_z^t(\boldsymbol{\rho}) = \sum_{m=1}^{M_e} \sum_{n=1}^{N_0} a_{m,n} U_{m,n}(\boldsymbol{\rho}), \quad \frac{\partial H_z^t(\boldsymbol{\rho})}{\partial \mathbf{n}} = \sum_{m=1}^{M_e} \sum_{n=1}^{N_0} b_{m,n} U_{m,n}(\boldsymbol{\rho}) \quad (2)$$

where N_0 is the number of sub-domain basis functions on the boundary of a sub-domain. $U_{m,n}(\boldsymbol{\rho})$ is the nth rectangular pulse function on the boundary of sub-domain m. $[a_{m,1}, \ldots, a_{m,N_0}]^T$ and $[b_{m,1}, \ldots, b_{m,N_0}]^T$ are denoted as $|a_m\rangle$ and $|b_m\rangle$ respectively for concision, where the superscript 'T' denotes the transpose. After substituting (2) into (1), Equation (3) can be obtained by the Galerkin's procedure:

$$\begin{bmatrix} Z_0 & Z_1 & \ldots & Z_{M_e-1} \\ Z_{-1} & Z_0 & \ddots & \vdots \\ \vdots & \ddots & \ddots & Z_1 \\ Z_{1-M_e} & \ldots & Z_{-1} & Z_0 \end{bmatrix} \begin{bmatrix} a_1 \\ a_2 \\ \vdots \\ a_{M_e} \end{bmatrix} + \begin{bmatrix} Y_0 & Y_1 & \ldots & Y_{M_e-1} \\ Y_1^T & Y_0 & \ddots & \vdots \\ \vdots & \ddots & \ddots & Y_1 \\ Y_{M_e-1}^T & \ldots & Y_1^T & Y_0 \end{bmatrix} \begin{bmatrix} b_1 \\ b_2 \\ \vdots \\ b_{M_e} \end{bmatrix} = \begin{bmatrix} g_1 \\ g_2 \\ \vdots \\ g_{M_e} \end{bmatrix} \quad (3)$$

where the matrix blocks $[Z_m]$, $[Y_m]$ or $[Z_{-m}]$, $[Y_m]^T$ represent the mutual coupling between a sub-domain and the mth sub-domain from its right or left respectively. $[Z_0]$ and $[Y_0]$ represent the self-coupling.

The sizes of all the matrix blocks in (3) are $N_0 \times N_0$. The elements of $[Z_m]$ and $[Y_m]$ are

$$Z_m^{i,j} = \left\langle U_{m',i}, L_1(U_{m'+m,j}) \right\rangle, \; Y_m^{i,j} = \left\langle U_{m',i}, L_2(U_{m'+m,j}) \right\rangle \tag{4}$$

where $L_1(U) = U - \oint_\Gamma U \frac{\partial G}{\partial \mathbf{n}'} d\Gamma'$ and $L_2(U) = \oint_\Gamma UG d\Gamma'$. $Z_m^{i,j}$ and $Y_m^{i,j}$ are independent of m'. Because of the symmetry of the Green's function, the second matrix in (3) is symmetrical. The element of the exciting vector $|g_m\rangle$ of Sub-domain m is $g_m^i = \langle U_{m,i}, H_z^{inc} \rangle$.

2.2. Using the FDFD Method in Each Sub-domain

Without loss of generality, Sub-domain m is discussed. Sub-domain m is discretized with Yee's cells [7], and the vector $|\phi_m\rangle$ is used to represent the total field values at all nodes of the Yee's cells. The following two relationships exist between $|a_m\rangle$, $|b_m\rangle$ and the total field values at the nodes.

Relationship 1: The elements of $|a_m\rangle$ are the average values of H_z^t on the two outmost layers of the H_z^t nodes of the Yee's cells.

Relationship 2: The elements of $|b_m\rangle$ can be expressed by the tangential total electric field values on the outmost layer of the corresponding nodes of the Yee's cells.

By combining Relationship 1, Relationship 2 and the classical FDFD equations at the nodes of the Yee's cells, Equation (5) is obtained:

$$\begin{bmatrix} A_{1,1} & 0 & A_{1,3} \\ A_{2,1} & A_{2,2} & 0 \end{bmatrix} \begin{bmatrix} \phi_m \\ b_m \\ a_m \end{bmatrix} = 0 \tag{5}$$

Then the relationship between $|a_m\rangle$ and $|b_m\rangle$ can be derived from (5) as follow:

$$|b_m\rangle = [B]\,|a_m\rangle \tag{6}$$

where $[B] = [A_{2,2}]^{-1}[A_{2,1}][A_{1,1}]^{-1}[A_{1,3}]$. The matrix $[A_{2,2}]$ is just a diagonal matrix. If $[A_{1,1}]$ is large, the computation of $[A_{1,1}]^{-1}[A_{1,3}]$ can be replaced with solving the matrix equation $[A_{1,1}][A_{temp}] = [A_{1,3}]$, so the inverse of $[A_{1,1}]$ is avoid and the sparse characteristic is kept.

Because all the elements in the array are the same, Equation (6) should be satisfied on the boundary of each sub-domain, and this can be expressed as

$$\begin{bmatrix} b_1 \\ \vdots \\ b_{M_e} \end{bmatrix} = \begin{bmatrix} B & \dots & 0 \\ \vdots & \ddots & \vdots \\ 0 & \dots & B \end{bmatrix} \begin{bmatrix} a_1 \\ \vdots \\ a_{M_e} \end{bmatrix} \tag{7}$$

After substituting (7) into (3), Equation (8) is obtained:

$$\left(\left[Z'_{1-M_e}\right] + \ldots + \left[Z'_0\right] + \ldots + \left[Z'_{M_e-1}\right]\right)|a\rangle = |g\rangle \tag{8}$$

where $|a\rangle = [a_1, \ldots, a_{M_e}]^T$ and $|g\rangle = [g_1, \ldots, g_{M_e}]^T$. $[Z'_m]$ is

$$\left[Z'_m\right] = \begin{bmatrix} 0 & 0 & \ldots & 0 & Z^e_m & 0 & \ldots & \ldots & 0 & 0 \\ 0 & 0 & 0 & \ldots & 0 & Z^e_m & 0 & \ldots & \ldots & 0 \\ \vdots & \vdots & \ddots & \ddots & & \ddots & \ddots & \ddots & & \vdots \end{bmatrix} (m > 0) \tag{9}$$

The positions of non-zero matrix blocks of $[Z'_m]$ and the positions of those of $[Z'_{-m}]$ are symmetrical with respect to the diagonal line, which represent the mutual coupling between a sub-domain and the mth sub-domain from its right and between a sub-domain and the mth sub-domain from its left, respectively. $[Z'_0]$ represents the self-coupling. Because all the elements in the array are the same, each matrix in (8) includes only one corresponding kind of matrix block, which can be expressed as

$$\begin{cases} \left[Z^e_m\right] = [Z_m] + [Y_m]\,[B] & \text{for } \left[Z'_m\right] \\ \left[Z^e_{-m}\right] = [Z_{-m}] + [Y_m]^T\,[B] & \text{for } \left[Z'_{-m}\right] \end{cases} \tag{10}$$

2.3. Application of the ABF/DMM Technique

The ABF/DMM technique is applied to solve (8). For the sake of integrity of this paper, it is described as follow, which has double iterations:

Step 0 $|a\rangle^0 = \left[Z'_0\right]^{-1}|g\rangle$

Step 1 $|a\rangle^1_k = |a\rangle^0 - \left[Z'_0\right]^{-1}\left(\left[Z'_{-1}\right] + \left[Z'_1\right]\right)|a\rangle^1_{k-1}$

$k = 1, 2, 3, \ldots$

$\vdots$

Step n $\quad |a\rangle^n_k = |a\rangle^0 - \left[Z'_0\right]^{-1}\begin{pmatrix} \left[Z'_{-n}\right] + \ldots + \left[Z'_{-2}\right] \\ + \left[Z'_{-1}\right] + \left[Z'_1\right] + \left[Z'_2\right] \\ + \ldots + \left[Z'_n\right] \end{pmatrix}|a\rangle^n_{k-1}$

$k = 1, 2, 3, \ldots$

$\vdots$

Step N_i $\quad |a\rangle^{Ni}_k = |a\rangle^0 - \left[Z'_0\right]^{-1}\begin{pmatrix} \left[Z'_{-Ni}\right] + \ldots + \left[Z'_{-2}\right] \\ + \left[Z'_{-1}\right] + \left[Z'_1\right] + \left[Z'_2\right] \\ + \ldots + \left[Z'_{Ni}\right] \end{pmatrix}|a\rangle^{Ni}_{k-1}$

$k = 1, 2, 3, \ldots$

The script 'n' denotes Step n, and the script 'k' denotes the kth iteration in a step. In Step n, the iteration is carried out until a stopping condition is satisfied, and then the iteration of Step n+1 is carried out.

The formula in each step is only a Jacobi iteration and can be modified to a Gauss-Seidel iteration. Then without loss of generality, the iteration formula for updating the unknown expansion coefficients $|a_m\rangle$ on the boundary Γ_m is

$$|a_m\rangle_k^n = |a_m\rangle^0 - [Z_0^e]^{-1} \left\{ \sum_{m'=\max\{m-n,1\}}^{m-1} \left[Z_{m'-m}^e\right] |a_{m'}\rangle_k^n + \sum_{m'=m+1}^{\min\{m+n,M_e\}} \left[Z_{m'-m}^e\right] |a_{m'}\rangle_{k-1}^n \right\} \tag{11}$$

In fact, the elements of the column vectors of $[Z_0^e]^{-1}$ are the ABFs' expansion coefficients, which are expanded by rectangular pulse functions with these expansion coefficients. Here, an ABF's physical interpretation is the distribution of the field on the boundary of a sub-domain, which is excited by a unit delta source on its boundary. The following two error criterions ε_c and ε_l are used for the convergence in each iteration step and the global convergence respectively:

$$\varepsilon_c = \frac{\left\| |a\rangle_k^n - |a\rangle_{k-1}^n \right\|}{\left\| |a\rangle_{k-1}^n \right\|}, \quad \varepsilon_l = \frac{\left\| |a\rangle_1^{n+1} - |a\rangle^n \right\|}{\| |a\rangle^n \|} \tag{12}$$

$|a\rangle^n$ is the final result of the iteration of Step n. When the two error criterions are less than the given threshold values, the iterations stop.

In the method in this paper, the whole process is divided into two steps as follows:

In the first step, a matrix equation constructed with finite-difference equations in only one sub-domain needs to be solved, whose size is much smaller than the matrix equation in the classical full-domain FDFD method, and can be solved by a direct method.

In the second step, the matrix $[Z_0^e]^{-1}$ needs to be obtained firstly, whose size is $N_0 \times N_0$. It is small and can be obtained by a direct method. Then Equation (8) is solved, whose size is $M_e N_0 \times M_e N_0$. Equation (8) is improved to be highly diagonally dominant through the ABF/DMM technique so that it can be solved efficiently by the iterative method. Additionally, considering the periodic property of the array, $2N_i + 1$ matrices need to be stored in the process of solving the matrix Equation (8), whose sizes are all $N_0 \times N_0$.

3. NUMERICAL RESULTS

To compare the method in this paper with the classical full-domain FDFD method, an example of a dielectric cylinder linear array with 30

elements is provided. The geometry of the array is shown in Figure 2, and the gap between the elements is 0.2375λ. The incident angle (θ) is 45° and the side length of the Yee's cells is 0.0125λ. For the classical full-domain FDFD method, the uniaxial PMLs are used to truncate the computational domain, and the number of the layers is 12. For the method in this paper, the size of each sub-domain is $0.55\lambda \times 0.25\lambda$. Both the two methods are programmed with Matlab 7.0 and running in a P4 desktop computer (CPU: 3.2 GHz).

Firstly, the size of the computational domain of the classical full-domain FDFD method is $23\lambda \times 0.7\lambda$, and the radar cross section (RCS) obtained by it is given in Figure 3(a). The RCSs obtained by the method in this paper with the stopping condition ($\varepsilon_c \leq 1\%$, $\varepsilon_l \leq 1.5\%$) and with considering all mutual coupling ($\varepsilon_c \leq 0.004\%$) are also given in Figure 3(a), respectively. It can be seen that the three RCSs are consistent except at the angles near $\theta = 90°$ (see Figure 3(a)), where the RCS obtained by the classical full-domain FDFD method ascends, and is larger than the other RCSs. Secondly, the size of the computational domain of the classical full-domain FDFD method is extended to be $23\lambda \times 2.7\lambda$, and the RCS obtained by it is given in Figure 3(b), which is compared with the RCS obtained by the method in this paper with considering all mutual coupling ($\varepsilon_c \leq 0.004\%$). Now the RCS obtained by the classical full-domain FDFD method descends at the angles near $\theta = 90°$, and the two RCSs are in very good agreement (see Figure 3(b)). By comparing the two cases, it can be seen that the ascending at the angles near $\theta = 90°$ in the RCS obtained by the classical full-domain FDFD method in the first case is due to artificial error, and this error can be reduced by extending the computational domain of the classical full-domain FDFD method as shown in the second case. However, this remedy will increase the

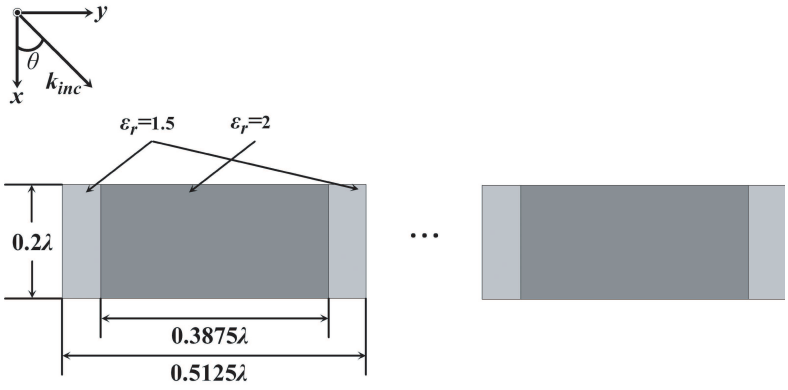

Figure 2. The geometry of a dielectric cylinder linear array.

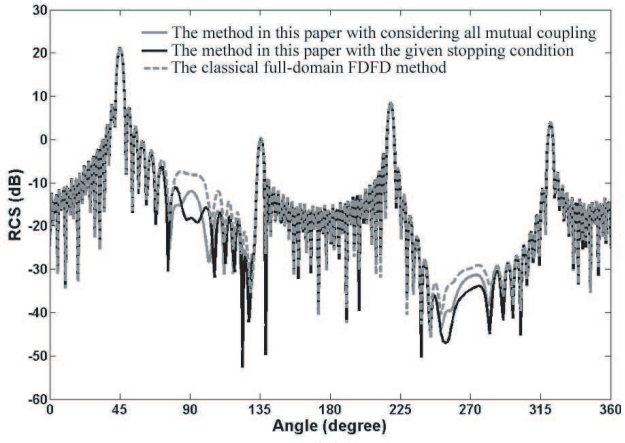

(a)

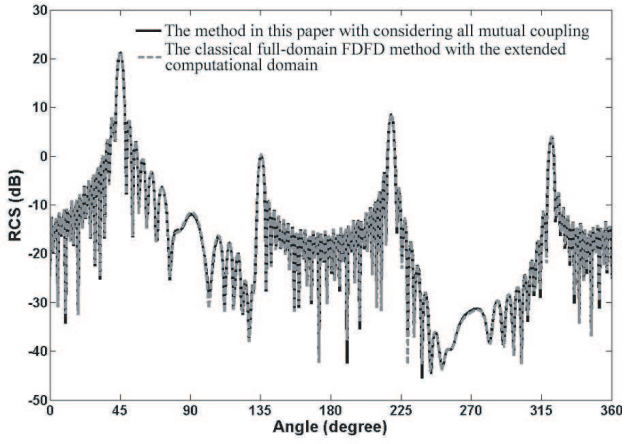

(b)

Figure 3. The RCSs of the array with 30 elements. (a) The size of the computational domain of the classical full-domain FDFD method is $23\lambda \times 0.7\lambda$. (b) The size of the computational domain of the classical full-domain FDFD method is extended to be $23\lambda \times 2.7\lambda$.

burden of computation rapidly. But this artificial error does not occur in the method in this paper. The total computational times are shown in Table 1, which are normalized with the computational time of the classical full-domain FDFD method with the extended computational domain, and it can be seen that the computational times of the method in this paper are largely less than that of the classical full-domain FDFD method, while the artificial error is avoided.

Table 1. Normalized computational time.

	Exact time	Normalized computational time
The classical full-domain FDFD method with the extended computational domain	1908 s	100%
The method in this paper with the given stopping condition ($\varepsilon_c \leq 1\%$, $\varepsilon_l \leq 1.5\%$)	147 s	7.7%
The method in this paper with considering all mutual coupling ($\varepsilon_c \leq 0.004\%$)	249 s	13.1%

4. CONCLUSION

In this paper, the combining scheme of the FDFD method and ABF/DMM technique is given for finite periodic linear arrays of inhomogeneous dielectric cylinders. Comparative numerical examples are given, in which some artificial error is observed in the classical full-domain FDFD method with PMLs. But in the method in this paper, no such problem occurs, and the computational time is largely reduced. Compared with the method in [5], the method in this paper does not need sample circles. The sample circles in the method in [5] may result in added computational domain in some cases, such as simulating flat cylinders. In the method in this paper, the boundary of the computational domain can be more close to objects, so it seems more flexible.

ACKNOWLEDGMENT

This work was supported by the Doctoral Program of Higher Education of China (No. 20060614005).

REFERENCES

1. Rappaport, C. M. and B. J. McCartin, "FDFD analysis of electromagnetic scattering in anisotropic media using unconstrained tri-

angular meshes," *IEEE Trans. Antennas Propag.*, Vol. 39, No. 3, 345–349, March 1991.

2. Norgren, M., "A hybrid FDFD-BIE approach to two-dimensional scattering from an inhomogeneous biisotropic cylinder," *Progress In Electromagnetics Research*, PIER 38, 1–27, 2002.
3. Wang, B.-Z., X. Wang, and W. Shao, "2D full-wave finite-difference frequency-domain method for lossy metal waveguide," *Microwave and Optical Technology Letters*, Vol. 42, No. 2, 158–161, July 2004.
4. Zhao, W., H. W. Deng, and Y. J. Zhao, "Application of 4-compnent compact 2-D FDFD method in analysis of lossy circular metal waveguide," *Journal of Electromagnetic Waves and Applications*, Vol. 22, No. 17–18, 2297–2308, December 2008.
5. Zheng, G. and B.-Z. Wang, "Analysis of scattering from multiple objects by the finite-difference frequency-domain method with an iteration-free multiregion technique," *IEEE Antennas and Wireless Propag. Letters*, Vol. 8, 794–797, 2009.
6. Zheng, G., B.-Z. Wang, H. Li, X.-F. Liu, and S. Ding, "Analysis of finite periodic dielectric gratings by the finite-difference frequency-domain method with the sub-entire-domain basis functions and wavelets," *Progress In Electromagnetics Reserch*, PIER 99, 453–463, 2009.
7. Talflove, A. and S. C. Hagness, *Computational Electrodynamics: The Finite-difference Time-domain Method*, Artech House, New York, 2000.
8. Waller, M. L. and S. M. Rao, "Application of adaptive basis functions for a diagonal moment matrix solution of arbitrarily shaped three-dimensional conducting body problems," *IEEE Trans. Antennas Propag.*, Vol. 50, No. 10, 1445–1452, October 2002.
9. Eshrah, I. A. and A. A. Kishk, "Analysis of linear arrays using the adaptive basis functions/diagonal moment matrix technique," *IEEE Trans. Antennas Propag.*, Vol. 53, No. 3, 1121–1125, March 2005.